Check for updates

Inducing high activity of a thermophilic enzyme at ambient temperatures by directed evolution†

Guangyue Li,[ab] Miguel A. Maria-Solano,[c] Adrian Romero-Rivera,[c] Sílvia Osuna [ID] *[c] and Manfred T. Reetz [ID] *[ab]

The long-standing problem of achieving high activity of a thermophilic enzyme at low temperatures and short reaction times with little tradeoff in thermostability has been solved by directed evolution, an alcohol dehydrogenase found in hot springs serving as the catalyst in enantioselective ketone reductions.

Robust enzymes derived from thermophilic organisms that thrive under extreme conditions as in hot springs are valuable catalysts in such processes as paper production, baking, laundry detergents and waste-treatment which operate at elevated temperatures.[1,2] At room temperature these enzymes generally show no activity or low turnover, which is inacceptable for other types of applications, as in the production of chiral pharmaceuticals or other fine chemicals.[3] For practical (industrial) applications, maximal stability and activity are needed, yet these appear to be opposing properties. Combining the virtues of pronounced enzyme robustness with high activity at ambient temperatures would lower energy expenditure and enable shorter reaction times under operating conditions, enabling high space-time yields.[3,4] A limited number of protein engineering studies of such thermostable enzymes using rational design or directed evolution based on mutator strains, epPCR and/or DNA shuffling have appeared.[5] The improvements proved to be moderate, generally with a tradeoff in thermostability.

The present study likewise focuses on increasing activity of a (hyper)thermally stable enzyme, but this time utilizing a different directed evolution technique. Our goal is opposite to that of conventional thermostabilization of mesophilic enzymes by directed evolution, the usual alternative that is generally accompanied by a tradeoff in activity. For example, Arnold *et al.* applied six cycles of random mutagenesis and DNA shuffling to the

p-nitrobenzyl esterase from *Bacillus subtilis* in order to enhance thermostability, the melting temperature (T_m) increasing from 57 °C to 71 °C, and the k_{cat}-value decreasing from 720 s^{-1} to 470 s^{-1} at 30 °C.[6] This kind of approach has been reviewed.[7] The mutational effects have been traced to protein rigidification due to newly introduced intramolecular H-bonds and salt bridges as well as disulfide bond formations. In the present approach the opposite effect can be anticipated, namely increased flexibility especially around the active site. Thus, a strategy complementary to the traditional approach would be of theoretical and practical interest. As will be seen, our results are also relevant to the current debate in evolutionary biology regarding changes of enzyme activity and stability starting from a hot environment to a cooled earth over a period of three billion years.[8]

As the model thermophilic enzyme we chose the NAD(P)H- and Zn-dependent alcohol dehydrogenase TbSADH[9,10] from *Thermoanaerobacter brockii*, first discovered in the hot springs of Yellowstone Park.[9a] It is identical to *Thermoanaerobacter ethanolicus* (TeSADH) from a different source, a previously used designation. In the purified form this ADH displays high thermostability as demonstrated by a half-life of 1.7 hours at 90 °C and 1.2 days at 80 °C.[9f] Thermostability as measured by differential scanning microcalorimetry is T_m = 98.5 °C.[9e] Using circular dichroism (CD), we determined T_m to be 90 °C, which is in the range of many hyperthermally stable enzymes.[5] It has been noted that in the reduction of a variety of structurally different ketones at ambient temperatures using this enzyme long reaction times of several days are needed,[9b] and keto-esters require 72 °C for reasonable conversion,[11a] as also reported for other thermophilic ADHs.[11b] In other cases, overnight reactions had to be performed.[9] In previous studies, protein engineering of TbSADH was applied for various purposes, including the increase and reversal of stereoselectivity for different substrates,[12] but a significant tradeoff in stability was often noted[12f,g] or thermostability was not measured.[12e]

The purpose of the present study was to evolve high activity of a thermophilic enzyme at low temperatures, enabling short reaction times for complete conversion while maintaining robustness.

[a] Max-Planck-Institut für Kohlenforschung, Kaiser-Wilhelm-Platz 1, 45470, Mülheim an der Ruhr, Germany

[b] Fachbereich Chemie der Philipps-Universität Marburg, Hans-Meerwein-Strasse, 35032, Marburg, Germany. E-mail: reetz@mpi-muelheim.mpg.de

[c] Institut de Química Computacional i Catàlisi and Department de Química, Universitat de Girona, Carrer Maria Aurèlia Capmany 6, Girona 17003, Catalonia, Spain. E-mail: silvia.osuna@udg.edu

† Electronic supplementary information (ESI) available. See DOI: 10.1039/c7cc05377k
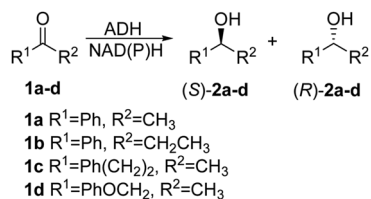
Scheme 1 Asymmetric reduction of ketones **1a–d** catalyzed by TbSADH mutants.

The TbSADH-catalyzed asymmetric reduction of acetophenone (**1a**) was chosen as the model system with enantioselectivity playing a secondary role (Scheme 1). Like many other thermo-stable ADHs,[13] TbSADH shows very low activity towards **1a** (and similar substrates)[9,11a] at 30 °C, and requires extended reaction times and more forcing conditions (e.g., overnight at 50–60 °C).[9] The wildtype (WT) is slightly (S)-selective (17–18% ee).[12g]

Two crystal structures of TbSADH have been reported,[10] one containing NAD(P)H which is the catalytically active form displaying an open binding pocket and a wide "entrance channel".[10a] We employed this structure (1YKF) in order to build a model for docking substrate **1a** into the binding pocket. In this way 13 residues were identified for potential saturation mutagenesis, 10 surrounding the substrate [C37, S39, A85, I86, L107, W110, T154, Y267, L294 and C295], and the rest occupying positions in the entrance channel [I49, C283 and M285] (Fig. 1). These positions were then subjected individually to NNK-based saturation mutagenesis in which all 20 canonical amino acids are used as combinatorial building blocks, requiring in each case the screening of ∼96 transformants for 95% library coverage.[14]
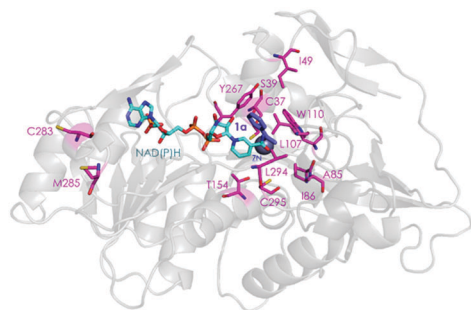

Fig. 1 TbSADH structure model showing docked acetophenone (**1a**) as substrate (in purple) based on the crystal structure of wildtype (1YKF),[8a] which served as a guide for choosing amino acid positions for saturation mutagenesis (in pink).

In the mini-libraries generated by randomization at positions 85, 86, 110, 283, 285 and 294, several mutants were discovered showing more than a 2-fold activity improvement, namely A85G, I86C, I86E, I86A, W110I, W110L, W110E, C283V, M285L, M285V, L294T and L294V. The libraries created at the other seven positions failed to harbor significantly improved variants (Table S1, ESI†). This information was then used as a basis for performing saturation mutagenesis at a relatively large 6-residue randomization site defined by the above hot spots. The use of NNK codon degeneracy would require for 95% library coverage the screening of $>10^9$ transformants.[14] As a practical alternative requiring only 1728 transformants, an appropriate reduced amino acid alphabet[14,15] was designed individually for each one of the six residues (Table S2, ESI†). The choice of the respective building blocks was guided by the amino acid substitutions that had shown positive effects in the initial NNK-based single libraries. This library harbored several distinctly improved variants (Table S3, ESI†), the best ones being TbSADH-1 (A85G/I86A) and TbSADH-2 (A85G/I86C) as shown by kinetic experiments using purified proteins (Table 1). At 30 °C the two variants show, relative to WT, 58- and 52-fold increases in k_{cat} and 301- and 61-fold improvements in catalytic efficiency (k_{cat}/K_m), respectively. At 45 °C, variants TbSADH-1 and TbSADH-2 also show notably better catalytic performance than WT, namely 51- and 36-fold increases in k_{cat} and improvements in k_{cat}/K_m by factors of 216 and 52-fold, respectively.

The best mutants TbSADH-1 and TbSADH-2 were tested in upscaled reactions at different temperatures using 50 mM of substrate **1a** in 1 mL of reaction volume (Table S4, ESI†). Excellent results were achieved, e.g., at 30 °C both variants ensured 96% conversion within 1.5 hour with complete enantio-selectivity (>99% ee (R)). In contrast, at the same temperature WT TbSADH required 20 hours for a mere 4% conversion and 17% ee (S). In further experiments, whole cell catalysis at 30 °C using TbSADH-1 and TbSADH-2 was successfully performed using substrate **1a** at concentrations ranging between 200 mM to 2 M (Table S5, ESI†).

We also measured the kinetics of WT TbSADH and variants TbSADH-1 and TbSADH-2 using ketones **1b–d**, revealing similar activity increases (Table S6, ESI†). Synthetically useful results were achieved once more, e.g., in the case of **1b** both variants reaching 96% conversion within one hour with 98% ee (R) (Table S7, ESI†). At the same temperature WT TbSADH led to less than 5% conversion after 20 hours with poor (S)-selectivity (27% ee).

The thermostability of both variants was measured by determining the melting temperature (T_m) using circular dichroism. Relative to WT TbSADH ($T_m = 90$ °C), the robustness of the two

Table 1 Kinetic results using acetophenone (**1a**) as substrate

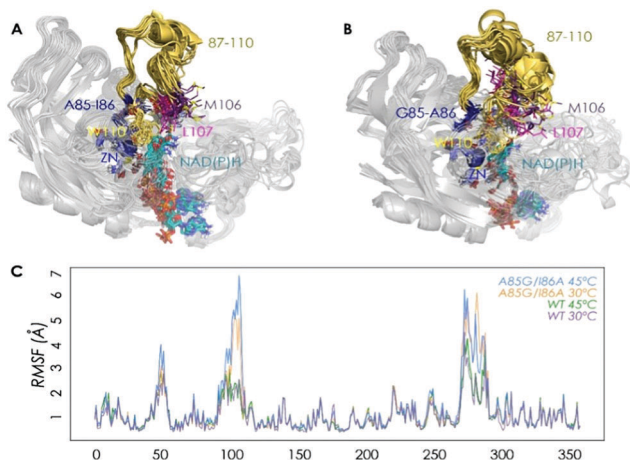|	Enzyme	Mutations	K_m (mM)	k_{cat} (min⁻¹)	k_{cat}/K_m (min⁻¹ M⁻¹)
30 °C	WT TbSADH		19.01 ± 1.68	1.80 ± 0.07	94
	TbSADH-1	A85G/I86A	3.70 ± 0.17	104.76 ± 1.31	28 313
	TbSADH-2	A85G/I86C	16.20 ± 2.46	93.15 ± 2.35	5750
45 °C	WT TbSADH		20.78 ± 1.25	3.79 ± 0.15	182
	TbSADH-1	A85G/I86A	4.95 ± 0.25	194.54 ± 3.14	39 301
	TbSADH-2	A85G/I86C	14.47 ± 2.05	136.04 ± 9.32	9402

Fig. 2 Overlay of representative snapshots for WT (A) and A85G/I86A variant (B) in the *apo* state at 30 °C. Average values of Root Mean Square Fluctuation (RMSF) of all residues computed from the MD simulations in the *apo* state (C).

best variants TbSADH-1 (T_m = 84 °C) and TbSADH-2 (T_m = 87.5 °C) is lowered by only 6 °C and 2.5 °C, respectively (Fig. S1 and Table S9, ESI†).

We then performed Molecular Dynamics (MD) simulations on the WT enzyme and the A85G/I86A variant, firstly for explaining the origin of dramatically enhanced activity at ambient temperature, and secondly to understand the reversed enantioselectivity (see ESI† for computational details). In Fig. 2 and Fig. S7 (ESI†), an overlay of representative snapshots from the MD simulations performed in the *apo* state is represented, together with the Root Mean Square Fluctuations (RMSF) of all residues at 30 and 45 °C. The analysis of RMSF allows us to identify the most flexible regions of the enzyme structure, and rationalize the effect of the A85G/I86A mutations on the TbSADH conformational dynamics. The loop composed of residues 87–110 that partially covers the active site of the enzyme (represented in yellow in Fig. 2A and B) is quite rigid in the case of the WT enzyme. The introduction of A85G/I86A induces a higher flexibility on the active site 87–110 loop, which is mainly due to a change in the backbone conformation of residues 106–107 as observed in the Ramachandran plot (see Fig. S8, and ESI† Movies). Residues 106–107 are located close to the active site, and make hydrophobic interactions with the substrate (see below). The change in the backbone conformation of 106–107 increases the volume of the active site (from *ca.* 96 Å^3 for WT to *ca.* 117 Å^3 for A85G/I86A), (Fig. S9 and Table S12, ESI†).

The higher flexibility of the A85G/I86A variant, especially in the active site loop, confers the enzyme the ability to change the shape of the active site easily and to adapt to the new non-natural substrate, thus leading to higher activity at low temperatures.

We have also performed MD simulations in the presence of acetophenone (**1a**) to elucidate the origin of reversed enantioselectivity as done in a previous study (see ESI† for details).[16] The higher flexibility of the active site loop 87–110 in the A85G/I86A variant plays a key role in dictating the enantioselectivity

of the process. In WT, L107 occupies the small binding pocket of the enzyme forcing **1a** to position the phenyl group in the large binding pocket. This orientation maximizes the CH···π and CH···CH interactions of **1a** and W110, L107, A85, and favors the *pro*-(*S*) pose. The higher flexibility of the active site loop in the A85G/I86A variant allows **1a** to position the phenyl ring in the small binding pocket, thus favoring the formation of the (*R*)-product. This *pro*-(*R*) orientation is stabilized by CH···π and CH···CH interactions between **1a** and residues W110, A86, and L294 (see Fig. S10 and S11, ESI†).

In conclusion, we have applied an efficient directed evolution strategy to evolve high activity of the thermophilic alcohol dehydrogenase TbSADH at ambient temperatures with little tradeoff in thermostability. Ketones such as acetophenone are rapidly reduced with pronounced enantioselectivity (99% ee) at ambient temperatures within short reaction times. The high thermostability of the mutant(s) suggests that further mutational changes if needed for other purposes can be tolerated.[17] The respective molecular phenomenon, uncovered by MD simulations, points to notably enhanced flexibility of an active site loop. A comparison of the movies of the wildtype and one of the mutants at the respective binding pockets nicely visualizes the underlying effect. This confers the active site pocket higher plasticity and the ability to adapt to new non-natural substrates at lower temperatures. Higher flexibility of the active site loop also has implications in the enantioselectivity of the process, as it changes the preferred orientation of the substrate in the active site pocket.

Our findings have bearing on a recent study in which the putative evolutionary drivers of thermoadaptation in enzyme catalysis were identified.[8a] On the basis of the hot-start hypothesis of ancestral proteins,[8] the authors note that "the challenge of evolving efficient enzymatic turnover at lower temperatures has not been addressed", emphasizing that the traditional concept of stability/activity tradeoff needs to be questioned in Darwinian evolution. While care must be taken when comparing natural with laboratory evolution, our results demonstrate the physical feasibility of evolving such mutational effects. On the practical side, the present mutagenesis approach needs to be generalized by including other (hyper)thermostable enzymes. It will be interesting to see if flexibilization around the binding pocket is a general phenomenon characteristic of such enzyme mutants.

Notes and references

1 Recent reviews of (hyper)thermophilic enzymes: (a) S. Elleuche, C. Schröder, K. Sahm and G. Antranikian, *Curr. Opin. Biotechnol.*, 2014, **29**, 116–123; (b) K. S. Siddiqui, *Biotechnol. Adv.*, 2015, **33**, 1912–1922; (c) P. A. Fields, Y. Dong, X. Meng and G. N. Somero, *J. Exp. Biol.*, 2015, **218**, 1801–1811; (d) N. Raddadi, A. Cherif, D. Daffonchio, M. Neifar and F. Fava, *Appl. Microbiol. Biotechnol.*, 2015, **99**, 7907–7913.

2 Reviews of applications of extremophiles: (a) J. G. Zeikus, C. Vieille and A. Savchenko, *Extremophiles*, 1998, **2**, 179–183; (b) M. E. Bruins, A. E. M. Janssen and R. M. Boom, *Appl. Biochem. Biotechnol.*, 2001, **90**, 155–186; (c) P. Falcicchio, M. Levisson, S. W. Kengen, S. Koutsopoulos and J. van der Oost, *Methods Mol. Biol.*, 2014, **1129**, 487–496; (d) F. Sarmiento, R. Peralta and J. M. Blamey, *Front. Bioeng. Biotechnol.*, 2015, **3**, 148; (e) N. Raddadi, A. Cherif, D. Daffonchio, M. Neifar and F. Fava, *Appl. Microbiol. Biotechnol.*, 2015, **99**, 7907–7913.

3 (a) A. S. Bommarius and B. Riebel, *Biocatalysis: Fundamentals and Applications*, Wiley-VCH, Weinheim, 2006; (b) *Industrial Biotransformations*, ed. A. Liese, K. Seelbach and C. Wandrey, Wiley-VCH, Weinheim, 2006; (c) K. Faber, *Biotransformations in Organic Chemistry*, Springer, Heidelberg, 6th edn, 2011; (d) *Enzyme Catalysis in Organic Synthesis*, ed. K. Drauz, H. Gröger and O. May, Wiley-VCH, Weinheim, 3rd edn, 2012; (e) *Organic Synthesis Using Biocatalysis*, ed. A. Goswani and J. Stewart, Elsevier, Amsterdam, 2015.

4 Reviews of process engineering and ecological aspects of biocatalysis:[3] (a) P. Tufvesson, J. Lima-Ramos, M. Nordblad and J. M. Woodley, *Org. Process Res. Dev.*, 2011, **15**, 266–274; (b) R. Sheldon, *Green Chem.*, 2017, **19**, 18–43; (c) M. Schrewe, M. K. Julsing, B. Bühler and A. Schmid, *Chem. Soc. Rev.*, 2013, **42**, 6346–6377; (d) Y. Ni, D. H. Holtmann and F. Hollmann, *ChemCatChem*, 2014, **6**, 930–943.

5 Examples of protein engineering of (hyper)thermophilic enzymes: (a) A. Merz, M.-C. Yee, H. Szadkowski, G. Pappenberger, A. Crameri, W. P. Stemmer, C. Yanofsky and K. Kirschner, *Biochemistry*, 2000, **39**, 880–889; (b) J. H. Lebbink, T. Kaper, P. Bron, J. van der Oost and W. M. de Vos, *Biochemistry*, 2000, **39**, 3656–3665; (c) A. Lönn, M. Gardonyi, W. van Zyl, B. Hahn-Hägerdal and R. C. Otero, *Eur. J. Biochem.*, 2002, **269**, 157–163; (d) D. Sriprapundh, C. Vieille and J. G. Zeikus, *Protein. Eng.*, 2003, **16**, 683–690; (e) H.-J. Kang, K. Uegaki, H. Fukada and K. Ishikawa, *Extremophiles*, 2007, **11**, 251–256; (f) C. Q. Zhong, S. Song, N. Fang, X. Liang, H. Zhu, X. F. Tang and B. Tang, *Biotechnol. Bioeng.*, 2009, **104**, 862–870; (g) C. M. Theriot, X. Du, S. R. Tove and A. M. Grunden, *Appl. Microbiol. Biotechnol.*, 2010, **87**, 1715–1726; (h) S. Hayashi, S. Akanuma, W. Onuki, C. Tokunaga and A. Yamagishi, *Biochemistry*, 2011, **50**, 8583–8593; (i) J. Zhang, H. Shi, L. Xu, X. Zhu and X. Li, *PLoS One*, 2015, **10**, e0133824.

6 (a) L. Giver, A. Gershenson, P.-O. Freskgard and F. H. Arnold, *Proc. Natl. Acad. Sci. U. S. A.*, 1998, **95**, 12809–12813; (b) F. H. Arnold, L. Giver, A. Gershenson, H. Zhao and K. Miyazaki, *Ann. N. Y. Acad. Sci.*, 1999, **870**, 400–403.

7 (a) V. G. Eijsink, S. Gåseidnes, T. V. Borchert and B. van den Burg, *Biomol. Eng.*, 2005, **22**, 21–30; (b) A. S. Bommarius and M. F. Paye, *Chem. Soc. Rev.*, 2013, **42**, 6534–6565; (c) M. J. Liszka, M. E. Clark, E. Schneider and D. S. Clark, *Annu. Rev. Chem. Biomol. Eng.*, 2012, **3**, 77–102.

8 (a) V. Nguyen, C. Wilson, M. Hoemberger, J. B. Stiller, R. V. Agafonov, S. Kutter, J. English, D. L. Theobald and D. Kern, *Science*, 2017, **355**, 289–294; (b) R. Wolfenden, *Cell. Mol. Life Sci.*, 2014, **71**, 2909–2915; (c) R. Nussinov and P. G. Wolynes, *Phys. Chem. Chem. Phys.*, 2014, **16**, 6321–6322.

9 Discovery and early studies of TeSADH/TbSADH: (a) R. J. Lamed and J. G. Zeikus, *Biochem. J.*, 1981, **195**, 183–190; (b) E. Keinan, E. K. Hafeli, K. K. Seth and R. Lamed, *J. Am. Chem. Soc.*, 1986, **108**, 162–169; (c) D. S. Burdette, C. Vieille and J. G. Zeikus, *Biochem. J.*, 1996, **316**, 115–122; (d) O. Bogin, M. Peretz, Y. Hacham, Y. Korkhin, F. Frolow, A. J. Kalb (Gilboa) and Y. Burstein, *Protein Sci.*, 1998, **7**, 1156–1163; (e) O. Bogin, M. Peretz, Y. Hacham, Y. Burstein, Y. Korkhin and F. Frolow, *Protein Sci.*, 1998, **7**, 1156–1163; (f) D. S. Burdette, V. Tchernajencko and J. G. Zeikus, *Enzyme Microb. Technol.*, 2000, **27**, 11–18; (g) C. Heiss and R. S. Phillips, *Chem. Soc., Perkin Trans.*, 2000, **16**, 2821–2825.

10 X-ray structures of TbSADH: (a) Y. Korkin, A. J. Kalb (Gilboa), M. Peretz, O. Bogin, Y. Burstein and F. Frolow, *J. Mol. Biol.*, 1998, **278**, 967–981; (b) C. Li, J. Heatwole, S. Soelaiman and M. Shoham, *Proteins: Struct., Funct., Genet.*, 1999, **37**, 619–627.

11 (a) D. Seebach, M. F. Züger, F. Giovanni, B. Sonnleitner and A. Fiechter, *Angew. Chem., Int. Ed. Engl.*, 1984, **23**, 151–152; (b) S. Diederichs, K. Linn, J. Lückgen, T. Klement, J.-H. Grosch, K. Honda, H. Ohtake and J. Büchs, *J. Mol. Catal. B: Enzym.*, 2015, **121**, 37–44.

12 Examples of mutagenesis studies of TbSADH: (a) C. Heiss, M. Laivenieks, G. Zeikus and R. S. Phillips, *J. Am. Chem. Soc.*, 2001, **123**, 345–346; (b) K. I. Ziegelmann-Fjeld, M. M. Musa, R. S. Phillips, J. G. Zeikus and C. Vieille, *Protein Eng., Des. Sel.*, 2007, **20**, 47–55; (c) R. Agudo, G.-D. Roiban and M. T. Reetz, *J. Am. Chem. Soc.*, 2013, **135**, 1665–1668; (d) J. M. Patel, M. M. Musa, L. Rodriguez, D. A. Sutton, V. V. Popik and R. S. Phillips, *Org. Biomol. Chem.*, 2014, **12**, 5905–5910; (e) C. M. Nealon, T. P. Welsh, C. S. Kim and R. S. Phillips, *Arch. Biochem. Biophys.*, 2016, **606**, 151–156; (f) Z. Sun, R. Lonsdale, A. Ilie, G. Li, J. Zhou and M. T. Reetz, *ACS Catal.*, 2016, **6**, 1598–1605; (g) Z. Sun, G. Li and M. T. Reetz, *Tet. Lett.*, 2016, **57**, 3648–3651.

13 Reviews of ADHs: (a) H. Gröger, W. Hummel, S. Borchert and M. Kraußer, in *Enzyme Catalysis in Organic Synthesis*, ed. K. Drauz, H. Gröger and O. May, Wiley-VCH, Weinheim, 3rd edn, 2012, pp. 1035–1110; (b) K. Götz, L. Hilterhaus and A. Liese, in *Enzyme Catalysis in Organic Synthesis*, ed. K. Drauz, H. Gröger and O. May, Wiley-VCH, Weinheim, 3rd edn, 2012, pp. 1205–1223; (c) T. S. Moody and J. D. Rozzell, in *Organic Synthesis Using Biocatalysis*, ed. A. Goswami and J. D. Stewart, Elsevier, Amsterdam, 2016, pp. 149–186.

14 Review of directed evolution of stereoselective enzymes with emphasis on iterative saturation mutagenesis: M. T. Reetz, *Angew. Chem., Int. Ed.*, 2011, **5**, 138–174.

15 (a) M. T. Reetz and S. Wu, *Chem. Commun.*, 2008, 5499–5501; (b) A. G. Sandström, Y. Wikmar, K. Engström, J. Nyhlen and J.-E. Bäckvall, *Proc. Natl. Acad. Sci. U. S. A.*, 2012, **109**, 78–83; (c) Z. Sun, Y. Wikmark, J.-E. Bäckvall and M. T. Reetz, *Chem. – Eur. J.*, 2016, **22**, 5046–5054.

16 (a) M. A. Maria-Solano, A. Romero-Rivera and S. Osuna, *Org. Biomol. Chem.*, 2017, **15**, 4122–4129; (b) A. Romero-Rivera, M. Garcia-Borràs and S. Osuna, *Chem. Commun.*, 2017, **53**, 284–297.

17 J. D. Bloom, S. T. Labthavikul, C. R. Otey and F. H. Arnold, *Proc. Natl. Acad. Sci. U. S. A.*, 2006, **103**, 5869–5874.